

A Top-Down Approach to Hierarchically Coherent Probabilistic Forecasting

Abhimanyu Das¹, Weihao Kong¹, Biswajit Paria², Rajat Sen¹
(ordered alphabetically)

¹Google Research, ²Carnegie Mellon University

{abhidas, senrajat, weihaokong}@google.com, bparia@cs.cmu.edu

Abstract

Hierarchical forecasting is a key problem in many practical multivariate forecasting applications - the goal is to obtain coherent predictions for a large number of correlated time series that are arranged in a pre-specified tree hierarchy. In this paper, we present a probabilistic top-down approach to hierarchical forecasting that uses a novel attention-based RNN model to learn the distribution of the proportions according to which each parent prediction is split among its children nodes at any point in time. These probabilistic proportions are then coupled with an independent univariate probabilistic forecasting model (such as Prophet or STS) for the root time series. The resulting forecasts are computed in a top-down fashion and are naturally coherent, and also support probabilistic predictions over all time series in the hierarchy. We provide theoretical justification for the superiority of our top-down approach compared to traditional bottom-up hierarchical modeling. Finally, we experiment on three public datasets and demonstrate significantly improved probabilistic forecasts, compared to state-of-the-art probabilistic hierarchical models.

1 Introduction

A central problem in multivariate time series modeling is the need to simultaneously forecast a group of possibly correlated time series arranged in a natural hierarchical structure. For example, in retail applications [Fildes et al., 2019], the time series may capture sales of items in a retailer’s inventory that can then be grouped into departments, categories and subcategories. In electricity demand forecasting [Van Erven and Cugliari, 2015], the time series may correspond to consumption at different granularities, starting with individual households, which could be progressively grouped into city-level, and then state-level consumption time-series. The hierarchical structure among the time series can usually be represented as a tree, with leaf-level nodes corresponding to time series at the finest granularity, while higher-level nodes represent coarser-granularities and are obtained by aggregating the values from its children nodes.

Since businesses often require forecasts at various different granularities (e.g. fine-grained forecasts for supply chain use-cases, and coarse-grained forecasts for marketing and strategy decisions), the goal is to build hierarchical forecasting models that can obtain accurate forecasts for time series at every level of the hierarchy. Furthermore, to ensure decision-making at different hierarchical levels are aligned, it is usually required to obtain predictions that are *coherent* [Hyndman et al., 2011] with respect to the hierarchy tree, that is, the forecasts of a parent time-series should be equal to the sum of forecasts of its children time-series. Finally, to facilitate better decision making, there is

an increasing shift in most forecasting applications towards probabilistic forecasting [Berrocal et al., 2010, Gneiting and Katzfuss, 2014]; that is, the forecasting model should quantify the uncertainty in the output and produce probabilistic predictions.

In this paper, we address the problem of obtaining coherent probabilistic forecasts for large-scale hierarchical time series. We propose a deep-learning based probabilistic top-down approach to hierarchical forecasting. It is scalable, can generate probabilistic predictions that are hierarchically coherent, and obtain state-of-the-art accuracy.

While several hierarchical forecasting approaches have been proposed in the past decade, probabilistic hierarchical forecasting approaches are much less common. Several hierarchical forecasting approaches [Hyndman et al., 2016, Taieb et al., 2017, Van Erven and Cugliari, 2015, Hyndman et al., 2016, Ben Taieb and Koo, 2019, Wickramasuriya et al., 2015, 2020, Panagiotelis et al., 2020] involve a two-stage process where the first stage involves generating independent (possibly incoherent) univariate base forecasts, followed by a second stage “reconciliation” step that adjusts these forecasts using the hierarchy structure, to finally obtain coherent predictions. These approaches are usually disadvantaged in terms of not having an end-to-end, joint optimization process for generating coherent multivariate forecasts. Furthermore, with the exception of Taieb et al. [2017], none of these approaches can directly handle probabilistic forecasts.

While none of the above methods use deep neural network architectures for hierarchical forecasting, there has recently been a large body of work on deep neural network models for multivariate forecasting [Salinas et al., 2020, Oreshkin et al., 2019, Rangapuram et al., 2018, Benidis et al., 2020, Sen et al., 2019], including probabilistic multivariate forecasting [Salinas et al., 2019, Rasul et al., 2021] and even graph neural network(GNN)-based models for forecasting on time series with graph-structure correlations [Bai et al., 2020, Cao et al., 2020, Yu et al., 2017, Li et al., 2017]. However, most of these works do not provide coherent predictions for hierarchical time series. To the best of our knowledge, the only work on a jointly-optimized deep-learning framework for coherent probabilistic forecasting is the recent work of Rangapuram et al. [2021], that offers a novel method for incorporating the reconciliation step as part of a deep neural network-based training process. Their approach is based on projecting the produced time series into a linear subspace that satisfies the hierarchical constraints.

In this paper, we present an alternate approach to probabilistic forecasting for hierarchical time series that is based on a decades-old method that has not received much recent attention: top-down forecasting. The basic idea is to first model the top-level forecast in the hierarchy tree, and then model the ratios or proportions according to how the top level forecasts should be distributed among the children time-series in the hierarchy. The resulting predictions are naturally coherent. Early top-down approaches proposed in the past were non-probabilistic, and were rather simplistic in terms of modeling the proportions; for example, by obtaining the proportions from historical averages [Gross and Sohl, 1990], or deriving them from independently generated (incoherent) forecasts of each time-series from another model [Athanasopoulos et al., 2009].

Crucially, our proposed model (and indeed all top-down approaches for forecasting) relies on the intuition that the top level time series in a hierarchy is usually much less noisy and less sparse, and hence much easier to predict. Furthermore, it is easier to predict proportions (that are akin to scale-free normalized time-series) at the lower level nodes than the actual time series themselves.

Our approach to top-down probabilistic forecasting involves modeling the proportions with an end-to-end deep learning model that jointly forecasts the proportions along which each parent time series is disaggregated among its children. We use a Dirichlet distribution [Olkin and Rubin,

1964] to model the distribution of proportions for each parent-children family in the hierarchy. The parameters of the Dirichlet distribution for each family is obtained from a Recurrent Neural Network (RNN) [Hochreiter and Schmidhuber, 1997] with multi-head self-attention [Vaswani et al., 2017], that is jointly learnt from all the time-series in the hierarchy.

The (univariate) root time series can be modeled independently using any univariate probabilistic forecasting approach - this versatility is an added benefit of our method. This can range from traditional methods like ARIMA, Structural Time Series [Harvey, 1990] and Generalized Additive Models [Hastie and Tibshirani, 1987] to probabilistic deep learning approaches [Salinas et al., 2020, Rangapuram et al., 2018]. In particular, we showcase results using two off-the-shelf univariate packages: Prophet [Taylor and Letham, 2018] and (the Tensorflow implementation [Dillon et al., 2017] of) Structural Time Series [Harvey, 1990] for the root.

The final probabilistic predictions for all the time series are obtained by composing the samples from the two probabilistic models (see Section 3 for more details).

1.1 Main contributions

Our main contributions are as follows:

Probabilistic top-down model. We propose a novel deep-learning based probabilistic top-model model that produces hierarchically-coherent probabilistic forecasts, without the need for a separate post-processing reconciliation step. The main component of our approach is an end-to-end RNN-based architecture that models (using a Dirichlet family) the proportions according to which parent time-series in the hierarchy disaggregates into their children at any point in time. This model can be coupled with any univariate probabilistic forecast for the root time series, to immediately obtain coherent probabilistic forecasts for the entire hierarchy tree. Furthermore, compared to the recent end-to-end deep-learning framework of [Rangapuram et al., 2021] which models the coherency constraints on the full batch of time series consisting of all the nodes of the hierarchy, our model is more scalable since it does not need to load all the time series in the hierarchy into each training mini-batch (see Section 3 for more details).

Theoretical justification. We theoretically analyze the advantage of the top-down approach (over a bottom-up approach) in a simplified linear regression setting for hierarchical prediction, and thereby provide theoretical justification for our top-down model. Specifically, we prove that for a 2-level hierarchy of d -dimensional linear regression with a single root node and K children nodes, the excess risk of the bottom-up approach is $\min(K, d)$ time bigger than the one of the top-down approach in the worst case. This validates our intuition that it is easier to predict proportions than the actual values themselves.

Empirical results. We validate the performance of our model against state-of-the art probabilistic hierarchical forecasting baselines on three public datasets, and demonstrate significant performance gains using our approach. We observe at least 6% relative improvement (and as much as 42% relative improvement) over baselines on CRPS scores.

1.2 Related work on hierarchical forecasting

As mentioned earlier, many existing coherent hierarchical forecasting methods rely on a two-stage reconciliation approach. This involves first generating independent, non-reconciled, base forecasts for all nodes in the tree, and then in a second stage, modifying or reconciling the forecasts using various optimization formulations to obtain the final, coherent forecasts. More specifically, at a

given time-step t , let $\mathbf{y}_t \in \mathbb{R}^n$ be the vector of all time series at all levels of the tree, $\mathbf{b}_t \in \mathbb{R}^m$ be the vector of only leaf time series, and $S \in \{0, 1\}^{n \times m}$ be the aggregation matrix representing the tree such that $\mathbf{y}_t = S\mathbf{b}_t$. Then given non-coherent base forecasts $\hat{\mathbf{y}}_t$, the goal of reconciliation approaches is to design a projection matrix $P \in \mathbb{R}^{m \times n}$ that can project the base forecasts linearly into new leaf forecasts, that are then aggregated using S to obtain (coherent) revised forecasts $\tilde{\mathbf{y}}_t = SP\hat{\mathbf{y}}_t$ (see, e.g., Section 2 of [Ben Taieb and Koo, 2019]). Different hierarchical methods specify different ways to optimize for the P matrix. The naive Bottom-Up approach [Hyndman and Athanasopoulos, 2018] simply aggregates up from the base leaf predictions to obtain revised coherent forecasts. The MinT method [Wickramasuriya et al., 2019] computes P that obtains the minimum variance unbiased revised forecasts, assuming unbiased base forecasts. The ERM method from Ben Taieb and Koo [2019] optimizes P by directly performing empirical risk minimization over the mean squared forecasting errors. Several other criteria [Hyndman et al., 2011, Van Erven and Cugliari, 2015] for optimizing for P have also been proposed. The PERMBU methods by Taieb et al. [2017] is the only reconciliation based hierarchical approach that provides probabilistic forecasts. The approach here is to start with independent marginal probabilistic forecasts for all nodes, then use samples from marginals at the leaf nodes, apply an empirical copula, and additionally perform a mean reconciliation step to obtain revised (coherent) samples for the higher level nodes.

The recent work of Rangapuram et al. [2021] is a single-stage end-to-end method that uses deep neural networks to obtain coherent probabilistic hierarchical forecasts. Their approach is to use a neural-network based multivariate probabilistic forecasting model to jointly model all the time series and explicitly incorporate a differentiable reconciliation step as part of model training, by using sampling and projection operations.

In addition to the coherent probabilistic forecasting approaches discussed above, several non-probabilistic and/or approximately coherent approaches have also been proposed in recent years. A lot of the methods are often aimed at using the hierarchy information for improving the accuracy of the predictions and not necessarily produce coherent predictions. Regularization based approaches [Mishchenko et al., 2019, Gleason, 2020] incorporate the hierarchy tree into the model via ℓ_2 regularization either on the predictions or node embeddings. Han et al. [2021a,b] similarly regularize the predictions to be coherent, and also extend it to forecasting quantiles. Another recently proposed approach by [Paria et al., 2021] consists of two parts, one coherent by design and another approximately coherent – based on the idea of decomposing the time series into a set of learned basis functions. While their model is scalable, it does not produce probabilistic forecasts.

2 Problem setting

We are given a set of N time-series arranged in a predefined hierarchy, each having T time points. We use $[N] := \{1, \dots, N\}$ to denote the set of time series indices. The time-series satisfy a coherence structure that will be defined later. The dataset can be represented by a matrix $\mathbf{Y} \in \mathbb{R}^{T \times N}$, where $\mathbf{y}^{(i)}$ denotes the i -th column, \mathbf{y}_t denotes the t -th row and $y_{t,i}$ the value at the sub-scripted index. Note that the subscript and the superscript can be replaced by set of time-points and a set of time-series indices respectively to denote the corresponding sub-matrices. We compactly denote the H -step history of \mathbf{Y} by $\mathbf{Y}_{\mathcal{H}} = [\mathbf{y}_{t-H}, \dots, \mathbf{y}_{t-1}]^\top \in \mathbb{R}^{H \times N}$ and the H -step history of $\mathbf{y}^{(i)}$ by $\mathbf{y}_{\mathcal{H}}^{(i)} = [\mathbf{y}_{t-H}^{(i)}, \dots, \mathbf{y}_{t-1}^{(i)}] \in \mathbb{R}^H$. Similarly we can define the F -step future as $\mathbf{Y}_{\mathcal{F}} = [\mathbf{y}_t, \dots, \mathbf{y}_{t+F-1}]^\top \in \mathbb{R}^{F \times N}$. We use the $\hat{\cdot}$ notation to denote predicted values.

Time series forecasts can often be improved by using external features or covariates that evolve with time, for example, categorical features such as *type of holiday*, or continuous features such as *time*

of the day. We denote the matrix of such features by $\mathbf{X} \in \mathbb{R}^{T \times D}$, where the t -th row denotes the D -dimensional feature vector at the t -th time step. For simplicity, we assume that the features are shared across all time series¹. We define $\mathbf{X}_{\mathcal{H}}$ and $\mathbf{X}_{\mathcal{F}}$ as above.

Coherency and Hierarchy: In many datasets (such as retail and traffic), the N time-series satisfy a coherence property defined by a hierarchical tree structure. The tree consists of a root node with several layers of descendents. For any non-leaf node $p \in [N]$ in the tree, let $\mathcal{L}(p)$ denote all its children time-series. In this case, the coherence property is given by,

$$\mathbf{y}^{(p)} = \sum_{i \in \mathcal{L}(p)} \mathbf{y}^{(i)}, \quad (\text{Coherence}) \quad (1)$$

and holds for all non-leaf nodes p . It follows that the time series for the root node is essentially the aggregation of all the leaf time series. Most hierarchical datasets are from retail and traffic applications [Wickramasuriya et al., 2020, Rangapuram et al., 2018] where the coherence property naturally arises and therefore we will work under that assumption.

Our *objective* is to accurately predict the distribution of the future $\hat{f}(\mathbf{Y}_{\mathcal{F}})$ such that any sample from the predicted distribution $\hat{\mathbf{Y}}_{\mathcal{F}} \sim \hat{f}(\mathbf{Y}_{\mathcal{F}})$ satisfies the coherence property in Eq. (1), given access to the data only upto time $t - 1$. Note that we will use \hat{f} and \hat{F} to denote the density and the cdf of the predictive distribution. Our objective is identical to the one defined by Rangapuram et al. [2021].

3 Probabilistic top-down model

In retail demand forecasting and traffic forecasting it is often the case that the time-series closer to the top level have more well defined seasonal pattern and trends, and therefore are more predictable. On the other hand as we go down the tree the time-series become sparser and more difficult to predict. This has been observed in prior works [Gross and Sohl, 1990, Athanasopoulos et al., 2009] and has led to top-down modeling being one of the popular methods.

In the top-down approach one predicts the top-level root time-series usually using traditional time-series forecasting methods and then the predictions are disaggregated down the hierarchy using historical proportions. In this paper we propose an end-to-end deep learning based top-down approach for disaggregating the parent time-series down the hierarchy. Our model can easily outperform historical proportions and provide probabilistic forecasts, when combined with any probabilistic forecasting model for the root node. Note that Hyndman et al. [2011] state that top-down forecasting cannot be unbiased under the assumption that base forecasts for all levels are independent. We do not generate base forecasts first and then reconcile and this independence assumptions does not apply to our setting.

Our model has two components: (i) a *top-down proportions* model for predicting the future proportions of the children for any parent node in the tree and (ii) a probabilistic forecasting model for the root. We first present the top-down proportions model, which is our main contribution.

Top-down proportions model: We propose a global top-down proportions model that predicts the future fractions/proportions according to which the future of any parent time-series disaggregates into its children time-series in the tree. This is based on the intuition that the proportions are more

¹Note that our modeling can handle both shared and time-series specific covariates in practice.

predictable given the history, as compared to the children time-series. Consider a *family* which is defined as a parent node p along with its children $\mathcal{L}(p)$. For any child $c \in \mathcal{L}(p)$, define

$$a_{s,c} = \frac{y_{s,c}}{\sum_{j \in \mathcal{L}(p)} y_{s,j}}, \quad \text{for all } s \in [T].$$

Thus, the resulting matrix $\mathbf{A}(p) \in \mathbb{R}^{T \times C}$ denotes the proportions of the children over time, where $C := |\mathcal{L}(p)|$. We will drop the p in braces when it is clear from context that we are dealing with a particular *family* $(p, \mathcal{L}(p))$. As in Section 2, we use $\mathbf{A}_{\mathcal{H}}$ and $\mathbf{A}_{\mathcal{F}}$ to denote the history and future proportions.

The task for our model is to predict the distribution of $\mathbf{A}_{\mathcal{F}}$ given the historical proportions $\mathbf{A}_{\mathcal{H}}$, the parent’s history $\mathbf{y}_{\mathcal{H}}^{(p)}$ and the covariates \mathbf{X} . Note that for any $s \in [T]$, $\mathbf{a}_s \in \Delta^{C-1}$, where Δ^{d-1} denotes the $(d-1)$ -dimensional simplex. Therefore, our predicted distribution should also be a distribution over the simplex for each row. Thus, we use the Dirichlet [Olkin and Rubin, 1964] family to model the output distribution for each row of the predicted proportions, as we will detail later.

Architecture. The two main architectural components that we use are (i) a LSTM based sequence to sequence (seq-2-seq) [Hochreiter and Schmidhuber, 1997] model to capture temporal structure and (ii) a multi-head self attention model [Vaswani et al., 2017] to capture the dependence across the children proportions. We first pass our inputs through the seq-2-seq model and obtain the decoder side output as follows,

$$\mathbf{D}_{\mathcal{F}} \leftarrow \text{seq2seq}(\mathbf{A}_{\mathcal{H}}, \mathbf{y}_{\mathcal{H}}^{(p)}, \mathbf{X}, \mathbf{E}^{(\mathcal{L}(p))})$$

where $\mathbf{E}^{(\mathcal{L}(p))}$ are embeddings for the children nodes that are jointly trained. The decoder output $\mathbf{D}_{\mathcal{F}}$ has shape $F \times C \times r$, where r denotes the output dimension of the decoder. Note that each child proportion time-series is fed independently to the seq-2-seq model i.e C is the batch dimension of the encoder-decoder, as shown in Figure 1. We then pass the decoder outputs through several layers of multi-headed self attention given by,

$$\mathbf{M}_{\mathcal{F}} \leftarrow \text{MultiHeadAtt}_{g,l}(\mathbf{D}_{\mathcal{F}}),$$

where g denotes the number of attention heads and l denotes the number of attention layers. Each attention layer is followed by a fully connected layer with ReLU activation and also equipped with a residual connection. Note that the attention is only applied across the third dimension i.e across the children. $\mathbf{M}_{\mathcal{F}}$ is of dimension $F \times C \times o$, where o is the output dimension of the attention layers. We finally pass this through a linear layer of output size one, with exponential link function to get an output $\mathbf{B}_{\mathcal{F}} \in \mathbb{R}_+^{F \times C}$ that is the same dimension as that of $\mathbf{A}_{\mathcal{F}}$. We provide a full illustration of our model in Figure 1.

Loss Function. Recall that the predicted proportions distributions $\hat{f}(\mathbf{A}_{\mathcal{F}})$ have to be over the simplex Δ^{C-1} for each of row. Therefore we model it by the Dirichlet family. In fact our final model output for a family $\mathbf{B}_{\mathcal{F}}$ represents the parameters of predictive Dirichlet distributions. Specifically, we minimize the loss

$$\ell(\mathbf{B}_{\mathcal{F}}, \mathbf{A}_{\mathcal{F}}) = -\frac{1}{F} \sum_{s=t}^{t+F-1} \text{DirLL}(\mathbf{a}_s + \epsilon; \mathbf{b}_s). \quad (2)$$

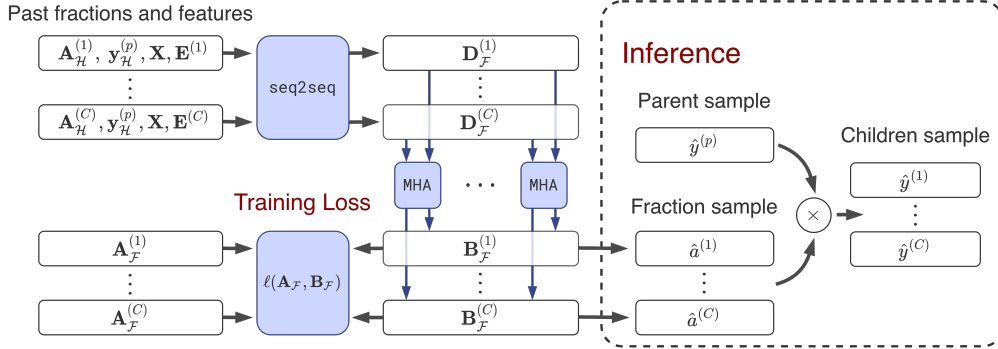


Figure 1: A complete description of the training and inference architecture is shown in the figure. MHA denotes multi-head self attention layers and seq2seq denotes any sequence to sequence model such as LSTM based encoder-decoder models. The indices $\{1, \dots, C\}$ are used to denote the indices of the children of parent node p . During inference the children fractions are sampled from the dirichlet distribution and multiplied with the parent to yield the children samples.

$\text{DirLL}(\mathbf{a}; \boldsymbol{\alpha})$ denotes the log-likelihood of Dirichlet distribution for target \mathbf{a} and parameters $\boldsymbol{\alpha}$.

$$\text{DirLL}(\mathbf{a}; \boldsymbol{\alpha}) := \sum_i (\alpha_i - 1) \log(a_i) - \log B(\boldsymbol{\alpha}), \quad (3)$$

where $B(\boldsymbol{\alpha})$ is the normalization constant. In Eq. (2), we add a small ϵ to avoid undefined values when the target proportion for some children are zero. In practice, we use Tensorflow Probability [Dillon et al., 2017] to optimize the above loss function.

Training. We train our top-down model with mini-batch gradient descent where each batch corresponds to different history and future time-intervals of the *same family*. For example, if the time batch-size is b and we are given a family $(p, \mathcal{L}(p))$ the input proportions that are fed into the model are of shape $b \times H \times C$ and the output distribution parameters are of shape $b \times F \times C$, where $C = |\mathcal{L}(p)|$. Note that we only need to load all the time-series of a given family into a batch as opposed to recently proposed deep learning methods like Rangapuram et al. [2018] that need to load all the time-series into GPU memory. The latter can be extremely prohibitive for large datasets.

Root probabilistic model: Given the trained *top-down proportions* we can generate the distribution of proportions for any internal family of the hierarchy. Thus, if we obtain probabilistic forecasts for the root time-series we can achieve our original objective in Section 2. The advantage of our method is that any uni-variate/multi-variate probabilistic forecasting model can be used for the root node. In this paper, we use two off-the-shelf univariate packages: Prophet [Taylor and Letham, 2018] and Structural Time Series ([Harvey, 1990] - available in Tensorflow Probability [Dillon et al., 2017]) for the root time series. The implementation details of the root probabilistic model can be found in Appendix C

Inference: At inference we have to output a representation of the predicted cumulative distribution $\hat{F}(\mathbf{Y}_{\mathcal{F}})$ such that the samples are reconciled as in Section 2. We can achieve this by sampling from the predictive distribution of the two trained models. For ease of illustration, we will demonstrate the procedure for one time point $s \in \{t, \dots, t + F - 1\}$.

We first sample $\hat{y}_s^{(r)}$ from the predictive distribution of the root node model. Then for every parent node (non leaf), p in the tree we generate a sample $\hat{\mathbf{a}}_s^{(\mathcal{L}(p))}$ that represents a sample of the predicted

children proportions for that family. The proportion samples and the root sample can be combined to form a reconciled forecast sample $\hat{\mathbf{y}}_s$. We can generate many such samples and then take empirical statistics to form the $\hat{F}(\mathbf{Y}_s)$, which is by definition reconciled.

4 Theoretical justification for the top-down approach

In this section, we theoretically analyze the advantage of the top-down approach over the bottom-up approach for hierarchical prediction in a simplified setting. Again, the intuition is that the root level time series is much less noisy and hence much easier to predict, and it is easier to predict proportions at the children nodes than the actual values themselves. As a result, combining the root level prediction with the proportions prediction actually yields a much better prediction for the children nodes. Consider a 2-level hierarchy of linear regression problem consisting of a single root node (indexed by 0) with K children. For each time step $t \in [n]$, a global covariate $\mathbf{x}_t \in \mathbb{R}^d$ is independently drawn from a Gaussian distribution $\mathbf{x}_t \sim \mathcal{N}(0, \Sigma)$, and the value for each node is defined as follows:

- The value of the root node at time t is $y_{t,0} = \theta_0^\top \mathbf{x}_t + \eta_t$, where $\eta_t \in \mathbb{R}$ is independent of \mathbf{x}_t , and satisfies $\mathbb{E}[\eta_t] = 0$, $\text{Var}[\eta_t] = \sigma^2$.
- A random K -dimensional vector $\mathbf{a}_t \in \mathbb{R}^K$ is independently drawn from distribution P such that $\mathbb{E}[a_{t,i}] = p_i$ and $\text{Var}[a_{t,i}] = s_i$, where $a_{t,i}$ is the i -th coordinate of \mathbf{a}_t . For the i -th child node, the value of the node is defined as $a_{t,i} \cdot y_{t,0}$.

Notice that for the i -th child node, $\mathbb{E}[y_{t,i} | \mathbf{x}_t] = p_i \theta_0^\top \mathbf{x}_t$, and therefore the i -th child node follows from a linear model with coefficients $\theta_i := p_i \theta_0$.

Now we describe the bottom-up approach and top-down approach and analyze the expected excess risk of them respectively. In the bottom-up approach, we learn a separate linear predictor for each child node separately. For the i -th child node, the ordinary least square (OLS) estimator is

$$\hat{\theta}_i^{\mathbf{b}} = \left(\sum_{t=1}^n \mathbf{x}_t \mathbf{x}_t^\top \right)^{-1} \sum_{t=1}^n \mathbf{x}_t y_{t,i},$$

and the prediction of the root node is simply the summation of all the children nodes.

In the top-down approach, a single OLS linear predictor

$$\hat{\theta}_0^{\mathbf{t}} = \left(\sum_{i=t}^n \mathbf{x}_t \mathbf{x}_t^\top \right)^{-1} \sum_{i=t}^n \mathbf{x}_t y_{t,0}$$

is firstly learnt for the root node, then the proportion coefficient $\hat{p}_i, i \in [K]$ is learnt for each node separately as

$$\hat{p}_i = \frac{1}{n} \sum_{t=1}^n \frac{y_{t,i}}{y_{t,0}}$$

and the final linear predictor for the i th child is $\hat{\theta}_i^{\mathbf{b}} = \hat{p}_i \hat{\theta}_0^{\mathbf{t}}$. Let us define the excess risk of an estimator $\hat{\theta}_i$ as $r(\hat{\theta}_i) = (\hat{\theta}_i - \theta_i)^\top \Sigma (\hat{\theta}_i - \theta_i)$. The expected excess risk of both approaches are summarized in the following theorem, proved in Appendix A.1.

Theorem 4.1 (Expected excess risk comparison between top-down and bottom-up approaches).
The total expected excess risk of the bottom-up approach for all the children nodes satisfies

$$\sum_{i=1}^K \mathbb{E}[r(\hat{\theta}_i^b)] \geq \sum_{i=1}^K (s_i + p_i^2) \frac{d}{n-d-1} \sigma^2,$$

and the total expected excess risk of the top-down approach satisfies

$$\begin{aligned} & \sum_{i=1}^K \mathbb{E}[r(\hat{\theta}_i^t)] \\ &= \frac{\sum_{i=1}^K s_i}{n} \theta_0^\top \Sigma \theta_0 + \left(\frac{\sum_{i=1}^K s_i}{n} + \sum_{i=1}^K p_i^2 \right) \frac{d}{n-d-1} \sigma^2, \end{aligned}$$

Applying the theorem to the case where the proportion distribution \mathbf{a}_t is drawn from a uniform Dirichlet distribution, we show the excess risk of the traditional bottom-up approach is $\min(K, d)$ times bigger than our proposed top-down approach in the following corollary. A proof of the corollary can be found in Appendix A.2

Corollary 4.2. *Assuming that for each time-step $t \in [n]$, the proportion coefficient \mathbf{a}_t is drawn from a K -dimensional Dirichlet distribution $\text{Dir}(\alpha)$ with $\alpha_i = \frac{1}{K}$ for all $i \in [K]$ and $\theta_0^\top \Sigma \theta_0 = \sigma^2$, then*

$$\frac{\mathbb{E}[\sum_{i=1}^K r(\hat{\theta}_i^b)]}{\mathbb{E}[\sum_{i=1}^K r(\hat{\theta}_i^t)]} = \Omega(\min(K, d)).$$

5 Experiments

We implement our probabilistic top-down model in Tensorflow [Abadi et al., 2016] and compare against multiple baselines on popular hierarchical time-series datasets.

Datasets. We experiment with two retail forecasting datasets, M5 [M5, 2020] and Favorita [Favorita, 2017], and Tourism-L [Tourism, 2019, Wickramasuriya et al., 2019] which is a dataset consisting of tourist count data. The history length and forecast horizon (H, F) were set to $(28, 7)$, $(28, 7)$ and $(24, 12)$, for Favorita, M5 and Tourism respectively. For M5 and Favorita we use the product hierarchy. For Tourism-L we benchmark on both the (Geo)graphic and (Travel) history based hierarchy. More details about the dataset and the features used for each dataset can be found in Appendix B. Note that for the sake of reproducibility, the tourism dataset and experimental setup is exactly the same as that in [Rangapuram et al., 2021]. We summarize the key features of the datasets in Table 1. These datasets are the largest among the popularly used public hierarchical forecasting datasets and therefore are ideal for benchmarking methods that are both scalable and accurate.

Model details. For our proportions model, we set the validation split to be of the same size as the test set, and immediately preceding it in time, which is standard [Rangapuram et al., 2018]. We tune several hyper-parameters using the validation set loss, the details of which are provided in Appendix D. Then we use the best hyper-parameter model to predict the Dirichlet parameters for proportions in the test set. We separately tune and train a Prophet model [Taylor and Letham, 2018] and Tensorflow Probability STS model [Abadi et al., 2016] on the training set for the root node time-series. Refer to Appendix C for more details on the root models. We then combine the

Table 1: Dataset features. The forecast horizon is denoted by F .

Dataset	Total time series	Leaf time series	Levels	Observations	F
M5	3060	3049	4	1913	7 days
Favorita	4471	4100	4	1687	7 days
Tourism-L (Geo)	111	76	4	228	12 months
Tourism-L (Trav)	445	304	5	228	12 months

predicted samples from the proportions model and root models in order to generate the predictive distribution quantiles for all time-series in the hierarchy, as detailed in Section 3. We refer to our overall models as TDPProb (Prophet)(when using Prophet for the root model) and TDPProb (STS)(when using STS for the root model).

Baselines. We compare our models above to the following coherent hierarchical forecasting baselines²:

1. Hier-E2E [Rangapuram et al., 2021] is an end-to-end deep-learning approach producing coherent probabilistic forecasts. We use the official implementation released by the authors publicly on Github³.
2. PERMBU-MINT [Taieb et al., 2017] is a copula based reconciliation approach for producing probabilistic hierarchical forecasts.
3. ETS-BU, ARIMA-BU are bottom up approaches, where base forecasts produced using ETS and ARIMA models are aggregated to produce aggregate level predictions.
4. ETS-MINT-OLS, ETS-MINT-SHR, ARIMA-MINT-OLS, ARIMA-MINT-SHR [Wickramasuriya et al., 2019] are MinT based reconciliation approaches on base forecasts produced using ETS and ARIMA. SHR corresponds to the covariance matrix with a shrinkage operator, and OLS denotes a diagonal covariance matrix as in ordinary least squares.
5. ETS-ERM, ARIMA-ERM [Ben Taieb and Koo, 2019] are ERM based methods applied to the base forecasts from ETS and ARIMA models. ERM does not assume the unbiasedness conditions as MinT [Wickramasuriya et al., 2019] and instead minimizes the empirical risk.
6. SHARQ [Han et al., 2021a] consists of an independent deep model which are trained sequentially one node at a time, and hence not scalable. The model outputs are regularized to enforce coherency.

We use the implementation released by Rangapuram et al. [2021] for running all the above baselines. Note that while the first two baselines are fully probabilistic, the prediction intervals for the rest of the baselines are obtained assuming normally distributed errors (see e.g. Section 3.5 of Hyndman and Athanasopoulos [2018]). We would also like to note that we were unsuccessful in running some of the baselines for some of the datasets using the officially released packages. In particular SHARQ experiments did not complete even after running for a week due to its sequential nature. Several of the other baselines returned invalid values, and hence were omitted from Tables 3 and 4.

Evaluation. We evaluate the forecasting accuracy using the continuous ranked probability score (CRPS). The CRPS [Gneiting and Raftery, 2007] is minimized when the predicted quantiles match the true distribution of the data. This is a popular metric to benchmark probabilistic forecasting [Rangapuram et al., 2018, Taieb et al., 2017].

²Note that these are the same baselines used by Rangapuram et al. [2018]

³<https://github.com/rshyamsundar/gluonts-hierarchical-ICML-2021>

Table 2: Normalized CRPS scores on Tourism-L across two hierarchies. We average the deep learning based methods over 10 independent runs. The rest of the methods had very little variance. We report the corresponding standard error and only bold the numbers that are significantly better than the rest. The second best numbers in each column are italicized. The mean is calculated over both the hierarchies. Rangapuram et al. [2018] had already distilled the best out of all considered baselines in their Table 4. For ease of comparison, we restate those numbers.

Tourism	L0	L1 (Geo)	L2 (Geo)	L3 (Geo)	L1 (Trav)	L2 (Trav)	L3 (Trav)	L4 (Trav)	Mean
TDProb (Prophet)	<i>0.0299</i> ± 0.0003	0.0781 ± 0.0013	0.1177 ± 0.0012	0.1642 ± 0.0014	<i>0.0946</i> ± 0.0035	0.141 ± 0.0027	0.2023 ± 0.0024	0.2698 ± 0.0023	0.1372
TDProb (STS)	0.0281 ± 0.003	0.078 ± 0.003	0.1179 ± 0.0021	0.1644 ± 0.0003	<i>0.0962</i> ± 0.0041	0.1415 ± 0.0027	0.2028 ± 0.0023	0.2702 ± 0.0022	<i>0.1410</i>
Hier-E2E	0.0810 ± 0.0053	0.1030 ± 0.0030	<i>0.1361</i> ± 0.0024	<i>0.1752</i> ± 0.0026	0.1027 ± 0.0062	0.1403 ± 0.0047	0.2050 ± 0.0028	0.2727 ± 0.0017	0.1520
Best of Rest	0.0438	<i>0.0816</i>	0.1433	0.2036	0.0830	<i>0.1479</i>	<i>0.2437</i>	<i>0.3406</i>	0.1609

Table 3: Normalized CRPS scores for the M5 dataset. We average the deep learning based methods over 10 independent runs. The rest of the methods had very little variance. We report the corresponding standard error and only bold numbers that are the statistically significantly better than the rest. The second best numbers in each column are italicized. Note: Some of the baselines listed in Sec. 5 returned invalid quantiles (NaNs) and were omitted from the table.

M5	L0	L1	L2	L3	Mean
TDProb (Prophet)	<i>0.0227</i> ± 0.0001	0.0273 ± 0.0004	0.0304 ± 0.0004	0.1992 ± 0.0006	0.0699 ± 0.0002
TDProb (STS)	0.0337 ± 0.0001	0.0356 ± 0.0002	0.0387 ± 0.0002	<i>0.2042</i> ± 0.0006	0.078 ± 0.0002
Hier-E2E	0.1143 ± 0.0039	0.1109 ± 0.0039	0.1175 ± 0.0039	0.2862 ± 0.003	0.1572 ± 0.0035
PERMBU-MINT	0.0224	<i>0.0281</i>	<i>0.0316</i>	0.2147	<i>0.0742</i>
ETS-BU	0.0386	0.0490	0.0536	0.2905	0.1079
ETS-MINT-OLS	0.0356	0.0457	0.0508	0.2853	0.1043
ETS-MINT-SHR	0.0408	0.0498	0.0539	0.2856	0.1075
ETS-ERM	0.3491	0.3502	0.3676	0.9406	0.5019
ARIMA-BU	0.1116	0.1127	0.1162	0.3006	0.1602
ARIMA-MINT-SHR	0.0671	0.0729	0.0752	0.2896	0.1262
ARIMA-ERM	0.0590	0.0616	0.0731	0.4043	0.1495

Table 4: Normalized CRPS scores for the Favorita dataset. We average the deep learning based methods over 10 independent runs. The rest of the methods had very little variance. We report the corresponding standard error and only bold numbers that are the statistically significantly better than the rest. The second best numbers in each column are italicized. Note: Some of the baselines listed in Sec. 5 returned invalid quantiles (NaNs) and were omitted from the table.

Favorita	L0	L1	L2	L3	Mean
TDProb (Prophet)	0.031 ± 0.0005	0.0503 ± 0.0005	0.0711 ± 0.0006	0.1478 ± 0.0009	0.0751 ± 0.0005
TDProb (STS)	0.0865 ± 0.0014	0.0992 ± 0.0014	<i>0.1114</i> ± 0.0014	0.1748 ± 0.0014	<i>0.118</i> ± 0.0013
Hier-E2E	<i>0.0635</i> ± 0.0027	<i>0.0944</i> ± 0.0023	0.1427 ± 0.0021	0.274 ± 0.0021	0.1437 ± 0.002
ETS-BU	0.0987	0.1061	0.1206	<i>0.1502</i>	0.1189
ETS-MINT-OLS	0.106	0.1135	0.1355	0.1669	0.1305
ARIMA-BU	0.0856	<i>0.0962</i>	0.1205	0.2199	0.1306
ARIMA-MINT-OLS	0.1266	0.1444	0.1504	0.2084	0.1574

Table 5: Normalized CRPS scores for an ablation study on the Favorita dataset. The first row corresponds to using the ground truth root value in the test window along with our proportions model. This is akin to looking into the future and is not achievable (signified by the different color).

Favorita Ablation	L0	L1	L2	L3	Mean
Ground truth root + predicted prop.	0.0 ± 0.0	0.0425 ± 0.0008	0.0706 ± 0.0012	0.1469 ± 0.0017	0.0657 ± 0.0009
TDProb (Prophet)	0.031 ± 0.0005	0.0503 ± 0.0005	0.0711 ± 0.0006	0.1478 ± 0.0009	0.0751 ± 0.0005
TDProb (Prophet) - No Attention	0.031 ± 0.0005	0.0547 ± 0.008	0.0778 ± 0.0015	0.1564 ± 0.0016	0.08 ± 0.0009
Prophet + historical fractions	0.031 ± 0.0005	0.061 ± 0.0	0.1036 ± 0.0	0.224 ± 0.0	0.1045 ± 0.0

Denote the F step q -quantile prediction for time series i by $\hat{Q}_{\mathcal{F}}^{(i)}(q) \in \mathbb{R}^F$. Then the CRPS loss is given by

$$\text{CRPS}(\hat{Q}_{\mathcal{F}}^{(i)}(q), \mathbf{Y}_{\mathcal{F}}^{(i)}) = \sum_s \int_0^1 2(\mathbb{I}[\mathbf{Y}_s^{(i)} \leq \hat{Q}_s^{(i)}(q)] - q)(\hat{Q}_s^{(i)}(q) - \hat{\mathbf{Y}}_s^{(i)})dq. \quad (4)$$

We report the CRPS scores of the prediction for each individual level of the hierarchy. Similar to Rangapuram et al. [2021], we also normalize the CRPS scores at each level, by the absolute sum of the true values of all the nodes of that level. We also report the mean of the level-wise scores denoted by *Mean* in Tables 2, 3 and 4.

We gather level wise performance of all the competing methods across all three datasets, as well as an ablation study for our method. We now present our results for each dataset.

M5: The results are presented in Table 3, where the best performing methods are bold and second best methods are italicized. The deep learning based methods are averaged over 10 runs while other methods had very little variance. We see that TDProb (Prophet) performs the best for all levels except L0, where PERMBU-MINT achieves the best CRPS. Overall in the mean column, TDProb (Prophet) performs the best, with PERMBU-MINT and TDProb (STS) close behind. In fact TDProb (Prophet) is around 6% better than the best baseline in the mean column. This shows that our proportions model can be coupled with strong off-the-shelf univariate forecasting models to achieve state-of-the-art performance. We hypothesize that Hier-E2E does not work well on these larger datasets because the DeepVAR model needs to be applied to thousands of time-series, which leads to a prohibitive size of the fully connected input layer and a hard joint optimization problem.

Favorita: The results are presented in Table 4, where we follow the same presentation convention as before. It can be seen that at L0, the Prophet model is the best, followed by Hier-E2E. In all rows, TDProb (Prophet) outperforms the other models by a large margin, resulting in a 42% better mean performance than the best (non-topdown) baseline. TDProb (STS) is the second best in the mean column even though the STS root model is worse than that of Hier-E2E.

Tourism: The Tourism-L dataset has two hierarchies and we train separate proportions model for the two hierarchies. In this dataset, we compare against all the baselines in [Rangapuram et al., 2021] in the exact same setting. We can see that both our models outperform the baselines across almost all levels and the mean column across two hierarchies, except for L1(Trav). TDProb (Prophet) is better than the rest of the (non-topdown) baselines by around 10%.

Ablation study. Finally, in Table 5 we dive deeper into the role of the various components in our proportions model for the Favorita dataset. The row deemed Ground truth root + predicted prop. is a moonshot benchmark that can look into the future i.e it uses ground-truth root predictions with

our proportions model. This showcases the accuracy that can be achieved when we have perfect root-level forecast. The second row is our actual TDProb (Prophet) model. The third row removes the decoder-side attention layer from TDProb (Prophet), and there is a drop in performance across all levels ($> L0$), thus showing the necessity of the attention mechanism. The last row corresponds to prediction using the root Prophet model combined with fixed historical proportions averaged over the last 28 days. It shows that our proportions model is significantly better than using historical proportions, especially at the lower levels.

6 Conclusion

In this paper, we proposed a probabilistic top-down based hierarchical forecasting approach, that obtains coherent, probabilistic forecasts without the need for a separate reconciliation stage. Our approach is built around a novel deep-learning model for learning the distribution of proportions according to which a parent time series is disaggregated into its children time series. Our model is flexible enough to be coupled with any univariate probabilistic forecasting method of choice for the root time series. It is also more scalable than previous deep-learning based probabilistic hierarchical forecasting approach in terms of training batch-size requirements. We show in empirical evaluation on several public datasets, that our model obtains state-of-the-art results compared to previous methods. We also provide some theoretical justification of the top-down approach in a simplified hierarchical linear prediction setting.

For future work, we plan to investigate joint optimization of root-level probabilistic models and proportions model within a single neural-network training framework. We also plan to explore how to extend our approach to handle more complex hierarchical structural constraints, beyond trees.

References

- Martín Abadi, Paul Barham, Jianmin Chen, Zhifeng Chen, Andy Davis, Jeffrey Dean, Matthieu Devin, Sanjay Ghemawat, Geoffrey Irving, Michael Isard, et al. Tensorflow: A system for large-scale machine learning. In *12th USENIX symposium on operating systems design and implementation (OSDI 16)*, pages 265–283, 2016.
- George Athanasopoulos, Roman A Ahmed, and Rob J Hyndman. Hierarchical forecasts for australian domestic tourism. *International Journal of Forecasting*, 25(1):146–166, 2009.
- Lei Bai, Lina Yao, Can Li, Xianzhi Wang, and Can Wang. Adaptive graph convolutional recurrent network for traffic forecasting. In H. Larochelle, M. Ranzato, R. Hadsell, M. F. Balcan, and H. Lin, editors, *Advances in Neural Information Processing Systems*, volume 33, pages 17804–17815. Curran Associates, Inc., 2020.
- Souhaib Ben Taieb and Bonsoo Koo. Regularized regression for hierarchical forecasting without unbiasedness conditions. In *Proceedings of the 25th ACM SIGKDD International Conference on Knowledge Discovery & Data Mining*, pages 1337–1347, 2019.
- Konstantinos Benidis, Syama Sundar Rangapuram, Valentin Flunkert, Bernie Wang, Danielle Maddix, Caner Turkmen, Jan Gasthaus, Michael Bohlke-Schneider, David Salinas, Lorenzo Stella, et al. Neural forecasting: Introduction and literature overview. *arXiv preprint arXiv:2004.10240*, 2020.

- Veronica J Berrocal, Adrian E Raftery, Tilmann Gneiting, and Richard C Steed. Probabilistic weather forecasting for winter road maintenance. *Journal of the American Statistical Association*, 105(490):522–537, 2010.
- Defu Cao, Yujing Wang, Juanyong Duan, Ce Zhang, Xia Zhu, Congrui Huang, Yunhai Tong, Bixiong Xu, Jing Bai, Jie Tong, and Qi Zhang. Spectral temporal graph neural network for multivariate time-series forecasting. In H. Larochelle, M. Ranzato, R. Hadsell, M. F. Balcan, and H. Lin, editors, *Advances in Neural Information Processing Systems*, volume 33, pages 17766–17778. Curran Associates, Inc., 2020.
- Joshua V Dillon, Ian Langmore, Dustin Tran, Eugene Brevdo, Srinivas Vasudevan, Dave Moore, Brian Patton, Alex Alemi, Matt Hoffman, and Rif A Saurous. Tensorflow distributions. *arXiv preprint arXiv:1711.10604*, 2017.
- Favorita. Favorita forecasting dataset. <https://www.kaggle.com/c/favorita-grocery-sales-forecast>, 2017.
- Robert Fildes, Shaohui Ma, and Stephan Kolassa. Retail forecasting: Research and practice. *International Journal of Forecasting*, 2019.
- Jeffrey L Gleason. Forecasting hierarchical time series with a regularized embedding space. *San Diego*, 7, 2020.
- Tilmann Gneiting and Matthias Katzfuss. Probabilistic forecasting. *Annual Review of Statistics and Its Application*, 1:125–151, 2014.
- Tilmann Gneiting and Adrian E Raftery. Strictly proper scoring rules, prediction, and estimation. *Journal of the American statistical Association*, 102(477):359–378, 2007.
- Charles W Gross and Jeffrey E Sohl. Disaggregation methods to expedite product line forecasting. *Journal of forecasting*, 9(3):233–254, 1990.
- Xing Han, Sambarta Dasgupta, and Joydeep Ghosh. Simultaneously reconciled quantile forecasting of hierarchically related time series. In *International Conference on Artificial Intelligence and Statistics*, pages 190–198. PMLR, 2021a.
- Xing Han, Jing Hu, and Joydeep Ghosh. Mecats: Mixture-of-experts for quantile forecasts of aggregated time series. *arXiv preprint arXiv:2112.11669*, 2021b.
- Andrew C Harvey. Forecasting, structural time series models and the kalman filter. 1990.
- Trevor Hastie and Robert Tibshirani. Generalized additive models: some applications. *Journal of the American Statistical Association*, 82(398):371–386, 1987.
- Sepp Hochreiter and Jürgen Schmidhuber. Long short-term memory. *Neural computation*, 9(8):1735–1780, 1997.
- Rob J Hyndman and George Athanasopoulos. *Forecasting: principles and practice*. OTexts, 2018.
- Rob J Hyndman, Roman A Ahmed, George Athanasopoulos, and Han Lin Shang. Optimal combination forecasts for hierarchical time series. *Computational statistics & data analysis*, 55(9):2579–2589, 2011.

- Rob J Hyndman, Alan J Lee, and Earo Wang. Fast computation of reconciled forecasts for hierarchical and grouped time series. *Computational statistics & data analysis*, 97:16–32, 2016.
- Yaguang Li, Rose Yu, Cyrus Shahabi, and Yan Liu. Diffusion convolutional recurrent neural network: Data-driven traffic forecasting. *arXiv preprint arXiv:1707.01926*, 2017.
- M5. M5 forecasting dataset. <https://www.kaggle.com/c/m5-forecasting-accuracy/>, 2020.
- Konstantin Mishchenko, Mallory Montgomery, and Federico Vaggi. A self-supervised approach to hierarchical forecasting with applications to groupwise synthetic controls. *arXiv preprint arXiv:1906.10586*, 2019.
- Ingram Olkin and Herman Rubin. Multivariate beta distributions and independence properties of the wishart distribution. *The Annals of Mathematical Statistics*, pages 261–269, 1964.
- Boris N Oreshkin, Dmitri Carпов, Nicolas Chapados, and Yoshua Bengio. N-beats: Neural basis expansion analysis for interpretable time series forecasting. *arXiv preprint arXiv:1905.10437*, 2019.
- Anastasios Panagiotelis, Puwasala Gamakumara, George Athanasopoulos, Rob J Hyndman, et al. Probabilistic forecast reconciliation: Properties, evaluation and score optimisation. *Monash econometrics and business statistics working paper series*, 26:20, 2020.
- Biswajit Paria, Rajat Sen, Amr Ahmed, and Abhimanyu Das. Hierarchically regularized deep forecasting. *arXiv preprint arXiv:2106.07630*, 2021.
- Syama Sundar Rangapuram, Matthias W Seeger, Jan Gasthaus, Lorenzo Stella, Yuyang Wang, and Tim Januschowski. Deep state space models for time series forecasting. *Advances in neural information processing systems*, 31:7785–7794, 2018.
- Syama Sundar Rangapuram, Lucien D Werner, Konstantinos Benidis, Pedro Mercado, Jan Gasthaus, and Tim Januschowski. End-to-end learning of coherent probabilistic forecasts for hierarchical time series. In *International Conference on Machine Learning*, pages 8832–8843. PMLR, 2021.
- Kashif Rasul, Abdul-Saboor Sheikh, Ingmar Schuster, Urs M Bergmann, and Roland Vollgraf. Multivariate probabilistic time series forecasting via conditioned normalizing flows. In *International Conference on Learning Representations*, 2021. URL <https://openreview.net/forum?id=WiGQBFuVRv>.
- David Salinas, Michael Bohlke-Schneider, Laurent Callot, Roberto Medico, and Jan Gasthaus. High-dimensional multivariate forecasting with low-rank gaussian copula processes. *arXiv preprint arXiv:1910.03002*, 2019.
- David Salinas, Valentin Flunkert, Jan Gasthaus, and Tim Januschowski. Deepar: Probabilistic forecasting with autoregressive recurrent networks. *International Journal of Forecasting*, 36(3): 1181–1191, 2020.
- Rajat Sen, Hsiang-Fu Yu, and Inderjit Dhillon. Think globally, act locally: A deep neural network approach to high-dimensional time series forecasting. *arXiv preprint arXiv:1905.03806*, 2019.
- Souhaib Ben Taieb, James W Taylor, and Rob J Hyndman. Coherent probabilistic forecasts for hierarchical time series. In *International Conference on Machine Learning*, pages 3348–3357. PMLR, 2017.

- Sean J Taylor and Benjamin Letham. Forecasting at scale. *The American Statistician*, 72(1):37–45, 2018.
- Tourism. Tourism forecasting dataset. <https://robjhyndman.com/publications/mint/>, 2019.
- Tim Van Erven and Jairo Cugliari. Game-theoretically optimal reconciliation of contemporaneous hierarchical time series forecasts. In *Modeling and stochastic learning for forecasting in high dimensions*, pages 297–317. Springer, 2015.
- Ashish Vaswani, Noam Shazeer, Niki Parmar, Jakob Uszkoreit, Llion Jones, Aidan N Gomez, Lukasz Kaiser, and Illia Polosukhin. Attention is all you need. In *NIPS*, 2017.
- Shanika L Wickramasuriya, George Athanasopoulos, Rob J Hyndman, et al. Forecasting hierarchical and grouped time series through trace minimization. *Department of Econometrics and Business Statistics, Monash University*, 105, 2015.
- Shanika L Wickramasuriya, George Athanasopoulos, and Rob J Hyndman. Optimal forecast reconciliation for hierarchical and grouped time series through trace minimization. *Journal of the American Statistical Association*, 114(526):804–819, 2019.
- Shanika L Wickramasuriya, Berwin A Turlach, and Rob J Hyndman. Optimal non-negative forecast reconciliation. *Statistics and Computing*, 30(5):1167–1182, 2020.
- Bing Yu, Haoteng Yin, and Zhanxing Zhu. Spatio-temporal graph convolutional networks: A deep learning framework for traffic forecasting. *arXiv preprint arXiv:1709.04875*, 2017.

A Proof

A.1 Proof of Theorem 4.1

We prove the claims about the excess risk of top-down and bottom-up approaches in the following two sections. Recall that ordinary least square (OLS) estimator $\hat{\theta} = \left(\sum_{i=1}^n \mathbf{x}_i \mathbf{x}_i^\top\right)^{-1} \sum_{i=1}^n \mathbf{x}_i y_i$. The population squared error of a linear predictor is defined as $(\hat{\theta} - \theta)^\top \Sigma (\hat{\theta} - \theta)$, which is also known as excess risk.

A.1.1 Excess risk of the top down approach

For the root node, the OLS predictor is written as

$$\hat{\theta}_0 = \left(\sum_{i=1}^n \mathbf{x}_i \mathbf{x}_i^\top\right)^{-1} \sum_{i=1}^n \mathbf{x}_i y_{i,0},$$

and the expected excess risk is

$$\begin{aligned} & \mathbb{E}[(\hat{\theta}_0 - \theta_0)^\top \Sigma (\hat{\theta}_0 - \theta_0)] \\ \stackrel{(a)}{=} & \mathbb{E} \left[\sigma^2 \sum_{i=1}^n \mathbf{x}_i^\top \left(\sum_i \mathbf{x}_i \mathbf{x}_i^\top\right)^{-1} \Sigma \left(\sum_i \mathbf{x}_i \mathbf{x}_i^\top\right)^{-1} \mathbf{x}_i \right] \\ \stackrel{(b)}{=} & \text{Tr} \left[\mathbb{E} \left[\sigma^2 \left(\sum_i \mathbf{x}_i \mathbf{x}_i^\top\right)^{-1} \Sigma \right] \right] \\ \stackrel{(c)}{=} & \sigma^2 d / (n - d - 1) \end{aligned} \tag{5}$$

where equation (a) holds by expanding $y_{i,0} = \mathbf{x}_i^\top \theta_0 + \eta_i$ and the fact that η_i is independent of \mathbf{x}_i , equation (b) holds by the property of trace, and equation (c) follows from the mean of the inverse-Wishart distribution.

For each children node, we learn the proportion coefficient with

$$\hat{p}_i = \frac{1}{n} \sum_{t=1}^n \frac{y_{t,i}}{y_{t,0}}.$$

Notice that

$$\begin{aligned} \text{Var}[\hat{p}_i] &= \frac{1}{n} \text{Var} \left[\frac{y_{1,i}}{y_{1,0}} \right] \\ &= \frac{1}{n} \text{Var}[a_i] \\ &= s_i / n. \end{aligned} \tag{6}$$

Recall that the optimal linear predictor of the i -th child node is $p_i \theta_0$. Therefore, the expected excess

risk of the top down predictor is

$$\begin{aligned}
& \mathbb{E} \left[(\hat{p}_i \hat{\theta}_0 - p_i \theta_0)^\top \Sigma (\hat{p}_i \hat{\theta}_0 - p_i \theta_0) \right] \\
&= \mathbb{E} \left[(\hat{p}_i \hat{\theta}_0 - p_i \hat{\theta}_0 + p_i \hat{\theta}_0 - p_i \theta_0)^\top \Sigma (\hat{p}_i \hat{\theta}_0 - p_i \hat{\theta}_0 + p_i \hat{\theta}_0 - p_i \theta_0) \right] \\
&= \mathbb{E} \left[(\hat{p}_i - p_i)^2 \hat{\theta}_0^\top \Sigma \hat{\theta}_0 + p_i^2 (\hat{\theta}_0 - \theta_0)^\top \Sigma (\hat{\theta}_0 - \theta_0) \right] \\
&\stackrel{(a)}{=} \frac{1}{n} s_i \theta_0^\top \Sigma \theta_0 + \left(\frac{1}{n} s_i + p_i^2 \right) \frac{d}{n-d-1} \sigma^2,
\end{aligned}$$

where we have applied Equation 6 and Equation 5 in equality (a). Taking summation over all the children, we get the total excess risk equals

$$\frac{\sum_{i=1}^K s_i}{n} \theta_0^\top \Sigma \theta_0 + \left(\frac{\sum_{i=1}^K s_i}{n} + \sum_{i=1}^K p_i^2 \right) \frac{d}{n-d-1} \sigma^2$$

A.1.2 Excess risk of the bottom up approach

For the i -th child node, the OLS estimator is

$$\hat{\theta}_i = \left(\sum_{t=1}^n \mathbf{x}_t \mathbf{x}_t^\top \right)^{-1} \sum_{t=1}^n \mathbf{x}_t y_{t,i}.$$

Recall that the best linear predictor of the i -th child node is $p_i \theta_0$. The excess risk is

$$\begin{aligned}
& \mathbb{E} (\hat{\theta}_i - p_i \theta_0)^\top \Sigma (\hat{\theta}_i - p_i \theta_0) \\
&= \mathbb{E} \left[((\hat{\theta}_i - p_i \hat{\theta}_0) + (p_i \hat{\theta}_0 - p_i \theta_0))^\top \Sigma ((\hat{\theta}_i - p_i \hat{\theta}_0) + (p_i \hat{\theta}_0 - p_i \theta_0)) \right]
\end{aligned}$$

Notice that the cross term has 0 expectation as

$$\begin{aligned}
& \mathbb{E} [(\hat{\theta}_i - p_i \hat{\theta}_0)^\top \Sigma (p_i \hat{\theta}_0 - p_i \theta_0)] \\
&\stackrel{(a)}{=} \mathbb{E} \left[\mathbb{E}_{\mathbf{a}} \left[\sum_{t=1}^n (a_{t,i} y_{t,0} - p_i y_{t,0}) \mathbf{x}_t^\top \left(\sum_{t=1}^n \mathbf{x}_t \mathbf{x}_t^\top \right)^{-1} \Sigma (p_i \hat{\theta}_0 - p_i \theta_0) \right] \right] \\
&\stackrel{(b)}{=} 0,
\end{aligned}$$

where the first equality holds by the definition of node i -th value $y_{t,i}$. Therefore, it holds that

$$\begin{aligned}
& \mathbb{E} \left[((\hat{\theta}_i - p_i \hat{\theta}_0) + (p_i \hat{\theta}_0 - p_i \theta_0))^\top \Sigma ((\hat{\theta}_i - p_i \hat{\theta}_0) + (p_i \hat{\theta}_0 - p_i \theta_0)) \right] \\
&= \mathbb{E} \left[(\hat{\theta}_i - p_i \hat{\theta}_0)^\top \Sigma (\hat{\theta}_i - p_i \hat{\theta}_0) \right] + p_i^2 \frac{d}{n-d-1} \sigma^2 \\
&= \mathbb{E} \operatorname{Tr} \left[\sum_{j=1}^n (a_{j,i} - p_i)^2 y_{t,0}^2 \mathbf{x}_j \mathbf{x}_j^\top \left(\sum_{t=1}^n \mathbf{x}_t \mathbf{x}_t^\top \right)^{-1} \Sigma \left(\sum_{t=1}^n \mathbf{x}_t \mathbf{x}_t^\top \right)^{-1} \right] + p_i^2 \frac{d}{n-d-1} \sigma^2 \\
&= s_i \mathbb{E} \operatorname{Tr} \left[\sum_{j=1}^n \left((\theta_0^\top \mathbf{x}_j)^2 + \eta_j^2 \right) \mathbf{x}_j \mathbf{x}_j^\top \left(\sum_{t=1}^n \mathbf{x}_t \mathbf{x}_t^\top \right)^{-1} \Sigma \left(\sum_{t=1}^n \mathbf{x}_t \mathbf{x}_t^\top \right)^{-1} \right] + p_i^2 \frac{d}{n-d-1} \sigma^2 \\
&\stackrel{(a)}{\geq} s_i \sigma^2 \mathbb{E} \operatorname{Tr} \left[\left(\sum_{j=1}^n \mathbf{x}_j \mathbf{x}_j^\top \right) \left(\sum_{t=1}^n \mathbf{x}_t \mathbf{x}_t^\top \right)^{-1} \Sigma \left(\sum_{t=1}^n \mathbf{x}_t \mathbf{x}_t^\top \right)^{-1} \right] + p_i^2 \frac{d}{n-d-1} \sigma^2 \\
&\stackrel{(b)}{=} (s_i + p_i^2) \sigma^2 \frac{d}{n-d-1},
\end{aligned}$$

where inequality (a) holds since $(\theta_0^\top \mathbf{x}_j)^2$ term is non-negative, equality (b) holds by the property of inverse-Wishart distribution. Taking summation over all the children, we get the total excess risk is lower bounded by

$$\sum_{i=1}^K (s_i + p_i^2) \frac{d}{n-d-1} \sigma^2$$

This concludes the proof.

A.2 Proof of Corollary 4.2

In this section, we apply Theorem 4.1 to Dirichlet distribution to show that the excess risk of bottom-up approach is $\min(d, K)$ times higher than top-down approach for a natural setting.

Recall that a random vector \mathbf{a} drawn from a K -dimensional Dirichlet distribution $\operatorname{Dir}(\alpha)$ with parameters α has mean $\mathbb{E}[\mathbf{a}] = \frac{1}{\sum_{i=1}^K \alpha_i} \alpha$, and the variance $\operatorname{Var}[a_i] = \frac{\alpha_i(1-\alpha_i)}{\sum_{i=1}^K \alpha_i + 1}$. Let $\alpha_i = \frac{1}{K}$ for all $i \in [K]$, $\theta_0^\top \Sigma \theta_0 = \sigma^2$. The total excess risk of the top-down approach is

$$\begin{aligned}
\mathbb{E} \left[\sum_{i=1}^K r(\hat{\theta}_i^t) \right] &= \frac{\sum_{i=1}^K s_i}{n} \theta_0^\top \Sigma \theta_0 + \left(\frac{\sum_{i=1}^K s_i}{n} + \sum_{i=1}^K p_i^2 \right) \frac{d}{n-d-1} \sigma^2 \\
&= \left(\frac{1-1/K}{2n} + \left(\frac{1-1/K}{2n} + \frac{1}{K} \right) \frac{d}{n-d-1} \right) \sigma^2.
\end{aligned}$$

The total excess risk of the bottom-up approach is lower bounded by

$$\begin{aligned}
\mathbb{E} \left[\sum_{i=1}^K r(\hat{\theta}_i^b) \right] &= (s_i + p_i^2) \frac{d}{n-d-1} \sigma^2 \\
&= \left(\frac{1-1/K}{2} + \frac{1}{K} \right) \frac{d}{n-d-1} \sigma^2
\end{aligned}$$

Now assuming that $n \geq 2d$, the top-down approach has expected risk $\mathbb{E}[\sum_{i=1}^K r(\hat{\theta}_i^t)] = O(\frac{1}{n} + \frac{d}{nK})$, and the bottom-up approach has expected risk $\mathbb{E}[\sum_{i=1}^K r(\hat{\theta}_i^t)] = \Omega(\frac{d}{n})$. Therefore, it holds that

$$\frac{\mathbb{E}[\sum_{i=1}^K r(\hat{\theta}_i^b)]}{\mathbb{E}[\sum_{i=1}^K r(\hat{\theta}_i^t)]} = \Omega(\min(d, K))$$

B Datasets

We use three publicly available benchmark datasets for our experiments.

1. The M5 dataset⁴ consists of time series data of product sales from 10 Walmart stores in three US states. The data consists of two different hierarchies: the product hierarchy and store location hierarchy. For simplicity, in our experiments we use only the product hierarchy consisting of 3k nodes and 1.8k time steps. Time steps 1907 to 1913 constitute a test window of length 7. Time steps 1 to 1906 are used for training and validation.
2. The Favorita dataset⁵ is a similar dataset, consisting of time series data from Corporación Favorita, a South-American grocery store chain. As above, we use the product hierarchy, consisting of 4.5k nodes and 1.7k time steps. Time steps 1681 to 1687 constitute a test window of length 7. Time steps 1 to 1686 are used for training and validation.
3. The Australian Tourism dataset⁶ consists of monthly domestic tourist count data in Australia across 7 states which are sub-divided into regions, sub-regions, and visit-type. The data consists of around 500 nodes and 228 time steps. This dataset consists of two hierarchies (Geo and Trav) as also followed in [Rangapuram et al., 2021]. Time steps 1 to 221 are used for training and validation. The test metrics are computed on steps 222 to 228.

For both M5 and Favorita we used time features corresponding to each day including day of the week and month of the year. We also used holiday features, in particular the distance to holidays passed through a squared exponential kernel. In addition, for M5 we used features related to SNAP discounts, and features related to oil prices for Favorita. For tourism we only used month of the year as a feature. All the input features were normalized to -0.5 to 0.5.

C Root Probabilistic Model

In this section, we provide more details about the implementation of our root probabilistic model using and Prophet [Taylor and Letham [2018]] and Structural Time Series [Harvey [1990]]. In the Prophet models for M5 and Favorita datasets, we combined three models implemented by Prophet: local linear trend with automatic change point detection, linear regression for holiday effect, and Fourier series for seasonality effect. The seasonality model include weekly seasonality, monthly seasonality, and yearly seasonality. In the Prophet model for Australian Tourism dataset, we combined local linear trend with automatic change point detection and Fourier series for seasonality effect, where the seasonality effect is on “month of year”. We tuned hyperparameters *seasonality prior scale*, *holidays prior scale*, *changepoint prior scale* and *Fourier orders* using the validation set.

In the Structural Time Series([Harvey [1990]](STS) model for M5 and Favorita datasets, we combined three models implemented in STS package in Tensorflow: local linear trend, autoregressive for

⁴<https://www.kaggle.com/c/m5-forecasting-accuracy/>

⁵<https://www.kaggle.com/c/favorita-grocery-sales-forecasting/>

⁶<https://robjhyndman.com/publications/mint/>

residual, linear regression for holiday effect, and seasonal effect model. The seasonality model include weekly seasonality and monthly seasonality. In the STS model for Australian Tourism dataset, we combined local linear trend, autoregressive and seasonality effect model, where the seasonality effect is on “month of year”. No hyperparameter tuning is done for the STS model.

D Additional Model Details

Hyper-parameters and validation. The hyper-parameters used in our proportions models are learning rate (log scale 1e-5 to 0.1), number of attention layers ([1, 2, 4, 6]), number of attention heads ([1, 2, 4, 6]), LSTM hidden size ([16, 32, 48, 64]), batch-size ([4, 8, 32, 64]), output hidden layer after LSTM decoder (ff-dim) ([32, 64, 256]), node embedding dimension ([4, 8, 16]). We tune these hyperparams on validation loss.

The best hyperparameters for the different datasets are:

Favorita. learning-rate: 0.00085, fixed-lstm-hidden: 48, num-attention-heads: 16, num-attention-layers: 2, ff-dim: 16, node-emb-dim: 4, batch-size: 32

M5. learning-rate: 0.00079, fixed-lstm-hidden: 48, num-attention-heads: 4, num-attention-layers: 6, ff-dim: 64, node-emb-dim: 8, batch-size: 4

Tourism. learning-rate: 0.00031, fixed-lstm-hidden: 32, num-attention-heads: 8, num-attention-layers: 4, ff-dim: 32, node-emb-dim: 16, batch-size: 48

Training details. Our model is implemented in Tensorflow [Abadi et al., 2016] and trained using the Adam optimizer with default parameters. We set a step-wise learning rate schedule that decays by a factor of 0.5 a total of 8 times over the schedule. The max. training epoch is set to be 50 while we early stop with a patience of 10.